Decoding the Conformational Binding of Drug Mixtures on Ovalbumin: An Integrated Multimodal Network

Michael González-Durruthy[1,2,*], Ramón Rial[1], Juan M. Ruso[1]

[1]Soft Matter and Molecular Biophysics Group, Department of Applied Physics and Institute of Materials (iMATUS), University of Santiago de Compostela, 15782 Santiago de Compostela, Spain.

[2]NanoSafety Group, International Iberian Nanotechnology Laboratory, Braga, 4715-330, Portugal. (M.G-D currently belongs to NanoSafety Group).

*Corresponding author

E-mail address: gonzalezdurruthy.furg@gmail.com and michael.gonzalez-durruthy@inl.int

Abstract

This research addresses the crucial necessity for a deeper understanding of the binding interactions between surfactants and proteins, with a specific focus on ovalbumin. Considering ovalbumin's role in diverse biochemical processes, it remains a subject of significant interest for drug discovery and design. To fill existing knowledge gaps, we investigated the binding interaction between dicloxacillin and cetyltrimethylammonium bromide (CTAB) on ovalbumin, employing a comprehensive approach that combines computational modeling with experimental validations. Using the ezPocket tool, the computational phase predicted ten relevant binding sites on ovalbumin's surface. The isobologram combination index (CI) heatmap strongly suggested a complex interplay of antagonistic and synergistic effects. Besides, a conformational drug-drug interaction network was proposed to explore the stability of the surfactant mixture within specific binding sites of ovalbumin, revealing a dynamic landscape of suggested antagonist effects. Experimental validations through UV-vis, Fluorescence, and circular dichroism (CD) spectroscopy further corroborated the computational findings, confirming the formation of stable complexes. Finally, this study not only advances our comprehension of ovalbumin's interactions with surfactants but also offers a multidimensional perspective and an advanced methodological framework for efficient therapeutic strategies, opening new avenues for future applications in drug development and applied biochemistry.

Keyworks: Ovalbumin, surfactant mixtures, molecular docking, conformational networks, spectrofluorimetric methods.

Highlights:

- Structure-based docking on surfactant mixture interactions.
- Building conformational binding network.
- Performed mechanistic isobolograms based combination index.
- Experimental spectrofluorimetric validation.

1. Introduction:

Proteins are key biomolecules with crucial roles in biological processes. Understanding their structure and interactions, especially in aqueous environments with molecules like surfactants, is essential for developing new therapeutic strategies. This knowledge is decisive for applications such as drug delivery, protein stabilization, and formulation development [1-3].

While protein-surfactant interactions have gained significant attention, the interactions involving protein-surfactant mixtures have been somewhat overlooked. Maldonado-Valderrama conducted thorough research on the interfacial characteristics of these mixtures, shedding light on their impact on interfacial tension, viscoelasticity, surface properties, and foam stability [4, 5]. Miller et al also delved into this area, specifically exploring ionic interactions and the influence of the isoelectric point. In this sense, they developed relevant theoretical models rooted in thermodynamics and statistical mechanics, capable of replicating experimental findings [6, 7].

On the other hand, pioneering papers explored the solubilization of solid protein-surfactant complex salts using a second surfactant in order to explore bulk properties of these systems, addressing the predominant influence of the catanionic associations over protein-surfactant interactions [8]. Another interesting study investigated the phase behavior in aqueous two-phase systems with cationic-anionic surfactant mixtures, highlighting the role of surfactant ratios, electrostatic interactions and providing molecular insights into protein partitioning, contributing to our understanding of phase separation mechanisms [9], or to discern the effect of the substitution of hydrogen atoms for fluorine atoms [10]. Also noteworthy is the method developed to create magnetic carbon nanotubes (MCNTs) that can bind and stabilize DNA and proteins using catanionic surfactants to enhance the electrostatic interaction between biomolecules and MCNTs, facilitating their rapid migration and compaction [11].

Within this research domain, ovalbumin (OVA), a major component of egg whites, emerges as a captivating protein because of its high content on essential amino acids which confer unique attributes beyond offering vital antimicrobial protection to the developing embryo [12, 13]. Ovalbumin has a primary structure consisting of a single polypeptide chain containing approximately 385 amino acid residues, with a molecular weight ranging from 45-50 kDa. Its secondary structure mainly adopts a α-helical conformation, with α-helices contributing approximately 60% of the secondary structure, thereby enhancing stability. Additionally, ovalbumin contains 1 disulfide bond that

enhance its stability by creating covalent linkages between specific cysteine residues (Cys87 and Cys133) within the polypeptide chain A [14, 15]. The ovalbumin's tertiary structure assumes a compact globular shape, which is stabilized by various non-covalent interactions, including hydrogen bonds, hydrophobic interactions, and van der Waals forces. Regarding all the points mentioned above, the physicochemical properties of ovalbumin have captured the interest of the scientific community, particularly in the context of interaction studies (including surfactant-drug mixtures studies), sparking curiosity among researchers in various scientific fields as food industry, biotechnology, pharmaceuticals, and drug development [16].

In this scenario, dicloxacillin (diclox) and CTAB are well-known surfactants that exhibit distinct characteristics and have been extensively studied individually. Dicloxacillin is a β-lactam penicillin-derivative well-known for its strong antibiotic properties, commonly used to treat infections caused by Gram-positive bacteria due to its ability to disrupt bacterial cell wall synthesis. While it is typically classified as a therapeutic drug or pharmacological agent, its amphiphilic nature has sparked interest in its potential surface-active properties from a purely chemical perspective [17]. On the other hand, cetyltrimethylammonium bromide (CTAB) is a versatile compound with diverse applications. From a chemical standpoint, CTAB is classified as a cationic surfactant, demonstrating a strong affinity for negatively charged groups from biomolecules, including proteins such as ovalbumin. Its high capacity to form micelles and interact with lipid membranes has led to its utilization in drug delivery and gene therapy [16]. Additionally, CTAB has been widely used in cosmetics and personal care products due to its emulsifying and conditioning effects. In molecular biology, CTAB is essential for DNA extraction, aiding in the separation of DNA from proteins and other cellular components. Furthermore, CTAB plays a pivotal role in material science, acting as a stabilizing agent in the synthesis of nanoparticles and nanomaterials to prevent particle aggregation. In the field of chemistry, CTAB serves as a cationic surfactant in various reactions, solubilizing a broad range of compounds in its micellar structures. This property facilitates chemical reactions and promotes the formation of organized assemblies, making CTAB valuable for applications such as thin film synthesis, nanomaterial templates, and the preparation of functional materials [18].

To study the interactions between ovalbumin and the dicloxacillin-CTAB mixture, a combined approach involving experimental techniques and heuristic computational methods was employed. This integration of experimental and computational approaches

presents several advantages. Primarily, it allows for the validation and cross-verification of the information obtained from both sources, thereby improving the reliability of the results. Secondly, it offers a multi-scale viewpoint, allowing the examination of both macroscopic characteristics and microscopic details concurrently. Among the experimental methods, ultraviolet-visible (UV-Vis) and fluorescence spectrometry have gained substantial prominence due to their adaptability, precision, and non-invasive properties in revealing the complexities of protein-surfactant interactions and highlighting the dynamic exchange between the molecules. Through integrating spectroscopic approaches, one can gain new insights into the structural, thermodynamic, and kinetic aspects of interactions between proteins and surfactants [19]. In recent years, computational techniques have become essential in elucidating complex interactions. Two techniques that have gained special attention are molecular docking simulations and Combination Index (CI) methodology, which can explore the binding mechanisms and thermodynamics of protein-surfactant as complex mixture [20]. With molecular docking simulations, one can predict the modes and strengths of protein-surfactant interactions [21]. Additionally, the CI methodology was employed to analyze the interaction between ovalbumin and the surfactant mixture. Our novel approach offers a strong theoretical and computational framework to determine whether these interactions are synergistic, additive, or antagonistic [20, 22-26]. We focus on the computational modeling aspects of our methodology to accurately quantify the subtle dynamics between the protein and the surfactant mixture. The use of theoretical isobolograms is essential to our analysis as they offer a graphical representation of the interaction patterns [20, 22-26].

This study could significantly contribute to boosting the knowledge of molecular interactions in such systems and makes a significant contribution to the field of surfactant-protein interactions. This understanding will aid in creating precise conformational models and theories about the behavior of ovalbumin in the presence of the dicloxacillin-CTAB mixture, advancing progress in drug design, biotechnological applications, and tailored surfactant development.

2. Materials and Methods.

2.1. Computational Approach.

2.1.1. Binding pockets predictions

Utilizing the ezPocket software, ten binding site cavities of the ovalbumin receptor (RCSB PDB ID: 1OVA) were well-identified. This software employs an algorithm rooted in Delaunay triangulation with weighted points and rapid Voronoi tessellation to analyze the protein's concave surfaces, pinpointing pertinent binding pockets. The algorithm employs a grid-based methodology to evaluate protein surface attributes, encompassing hydrophobicity, polarity, and morphology. Post-execution, the software yields ranked data on detected junction cavities, the central XYZ coordinates of these cavities, and their respective volumes. Concurrently, a 3D representation of all identified cavities is rendered for visualization. Herein, ten relevant binding sites were obtained as volumetric maps for the ovalbumin receptor allowing to set the specific three-dimensional discrete space as docking box simulations [27, 28] in each pockets as follow: *pocket 1* grid box size with dimensions of X = 20 Å, Y = 20 Å, Z = 20 Å and grid box center X = 5.65 Å, Y = 49.91 Å, Z = 37.56 Å, with volume equal to 11231.9 $Å^3$; *pocket 2* grid box size with dimensions of X = 20 Å, Y = 20 Å, Z = 20 Å and grid box center X = 13.68 Å, Y = 25.64 Å, Z = 43.33 Å, with volume equal to 1555.96 $Å^3$; *pocket 3* grid box size with dimensions of X = 20 Å, Y = 20 Å, Z = 20 Å and grid box center X = -4.06 Å, Y = 62.88 Å, Z = 40.73 Å, with volume equal to 1393.71 $Å^3$; *pocket 4* grid box size with dimensions of X = 20 Å, Y = 20 Å, Z = 20 Å and grid box center X = -20.52 Å, Y = 71.09 Å, Z = 41.15 Å, with volume equal to 1172.77 $Å^3$, *pocket 5* grid box size with dimensions of X = 20 Å, Y = 20 Å, Z = 20 Å and grid box center X = 9.22 Å, Y = 19.83 Å, Z = 30.54 Å, with volume equal to 887.56 $Å^3$; *pocket 6* grid box size with dimensions of X = 20 Å, Y = 20 Å, Z = 20 Å and grid box center X = -22.32 Å, Y = 55.94 Å, Z = 57.16 Å, with volume equal to 625.11 $Å^3$; *pocket 7* grid box size with dimensions of X = 20 Å, Y = 20 Å, Z = 20 Å and grid box center X = 31.39 Å, Y = 37.65 Å, Z = 31.30 Å, with volume equal to 602.04 $Å^3$; *pocket 8* grid box size with dimensions of X = 20 Å, Y = 20 Å, Z = 20 Å and grid box center X = -10.30 Å, Y = 23.92 Å, Z = 30.19 Å, with volume equal to 525.40 $Å^3$; *pocket 9* grid box size with dimensions of X = 20 Å, Y = 20 Å, Z = 20 Å and grid box center X = -22.15 Å, Y = 62.33 Å, Z = 31.96 Å, with volume equal to 508.45 $Å^3$; *pocket 10* grid box size with dimensions of X = 20 Å, Y = 20 Å, Z = 20 Å and grid box center X = 5.87 Å, Y = 82.75 Å, Z = 43.11 Å, with volume equal to 493.40 $Å^3$.

2.1.2. Molecular docking and conformational drug-drug interaction network

A molecular docking approach was executed by using AMDock, a software tailored for proficient prediction of protein-ligand binding modes and ΔG binding affinities (kcal/mol). AMDock's methodology amalgamates a genetic algorithm with a grid-based strategy.[29] The preliminary phase necessitated the preparation of the ovalbumin receptor and the ligand structures of the binary catanionic mixture, specifically dicloxacillin (PubChem CID: 18381; MW: 470.3 g/mol) and hexadecyltrimethylammonium bromide–CTAB (PubChem CID: 5974; MW: 364.4 g/mol) [30].

For the ovalbumin structure, co-crystalized ligands and water molecules were excised. The dicloxacillin and CTAB structures forming the mixture were primed by allocating Gasteiger charges and optimizing geometries. The AMDock algorithm employs a hybrid scoring function, amalgamating various energy force field terms, to assess the ligand's binding affinity across diverse orientations and conformations. For discerning the paramount binding mode based on individual ligand conformations (N = 10 conformations) and the binary mixture, AMDock adopts a hierarchical simulation protocol [29]. This commences with a coarse-grained search via an FFT-based technique, succeeded by a refinement phase leveraging a Monte Carlo algorithm. Subsequent to docking, the predicted conformational binding modes and ΔG affinities values undergo further scrutiny and validation through an array of post-docking analytical tools aiming to further construction of the conformational drug-drug interaction network in three simulation conditions i) dicloxacillin conformational drug-drug interaction network, ii) CTAB conformational drug-drug interaction network, and iii) mixture dicloxacillin plus CTAB conformational drug-drug interaction network [29].

2.1.3. Determining the mixture combination index (CI)

The Combination Index (CI) methodology was introduced to theoretically evaluate the drug combination binding effects (ie., antagonism or synergism) of a catanionic mixture formed by CTAB and dicloxacillin under interaction with each of the ten Ovalbumin binding pockets (numbered from θ = 1 to θ = 10) [22, 24-26, 31]. Within this computational framework, the foundational principle posits that two ligands or drugs exhibit synergistic binding affinity when their joint binding effect surpasses the cumulative effect of their individual binding contributions. Conversely, they display antagonistic binding affinity when their combined effect is less to their individual effects.

To ascertain CI values, it's imperative to assay various theoretical concentrations of each drug, both singularly and in tandem, and subsequently gauge the binding impact of the combination on the respective ovalbumin binding pockets. Given the theoretical docking simulation data, the CI for each catanionic ligand combination can be expressed according to the equation:

$$CI_{(CTAB-dicloxacillin)} = \sum_{\theta=1}^{\theta=10} \frac{C_{CTAB}}{C_{i\_CTAB}} + \frac{C_{dicloxacillin}}{C_{i\_dicloxacillin}} + \frac{C_{CTAB}C_{dicloxacillin}}{C_{i\_CTAB}C_{i\_dicloxacillin}} \quad (1)$$

Here, C_{CTAB} and $C_{dicloxacillin}$ represent the theoretical concentrations of CTAB and dicloxacillin in the catanionic mixture, respectively. Meanwhile, C_{i_CTAB} and $C_{i\_dicloxacillin}$ denote the theoretical concentrations of CTAB and dicloxacillin that yield an equivalent effect when administered individually. The CI value for the CTAB-dicloxacillin mixture binding combination spans from < 1 to > 1 and can be estimated as the summation of the mixture and individual binding contribution of the ligands (CTAB-dicloxacillin) with the all the pocket binding sites denoted by the parameter θ (i.e., covering form the site θ =1 to θ =10). From the mechanistic point of view, CI values < 1 can be associated to synergistic binding effect, CI values equal to 1 represent an additive binding effect, while CI values > 1 indicate an antagonistic binding effect. The obtained graph is called as theoretical isobologram representing a 2D matrix of drug-drug binding combination at a given theoretical concentration ranging from 0.0 mM to 1.0 mM. Theoretical isobolograms allow the visualization of the ligand interaction's nature its magnitude under combination conditions, such as in mixtures.

2.2. Experimental validation

2.2.1. Reagents

Hexadecyltrimethylammonium bromide (CTAB, 99%, ref. n. H5882), sodium dicloxacillin [3-(2,6 - dichlorophenyl)–5–methyl–4-Isoxazolyl penicillin] (ref. n. D9016) and ovalbumin (albumin, chicken egg, product A-5253, powder, molecular weight 44287 Da, 62-88% agarose gel electrophoresis, Sigma Chemical Company) were used without further purification. Samples were freshly prepared for each experiment within 1 h. prior to usage. Solutions were made using triple-distilled and degassed water.

2.2.2. UV-vis absorption spectra

UV-visible absorption spectra were obtained using a Cary 100 Bio UV-Vis Spectrophotometer within a wavelength range of 225 – 400 nm. A standard solution of ovalbumin, at a concentration of 1 mg/mL (equivalent to 0.07 mM), served as the reference for UV measurements. To assess the individual absorbance effects of each compound, solutions of pure dicloxacillin and CTAB were incrementally introduced in concentrations between 0.083 mM and 0.83 mM, ensuring a consistent ovalbumin concentration. According to the literature, the peak plasma concentration of dicloxacillin in standard dosage can reach up 0.2 mM [32]. Additionally, we aimed to investigate the impact of reaching the critical micelle concentration of CTAB, documented to be between 0.8 - 0.9 mM [33]. Hence, concentration interval was selected to align with both the plasma drug concentration range and the CMC of CTAB. Additionally, mixtures with equal concentrations of both ligands were introduced to the 0.07 mM protein solution. Each measurement was conducted in duplicate to validate accuracy and reduce potential errors. The observed replicates exhibited negligible variation, with the reported data reflecting the average of both measurements.

2.2.3. Fluorescence emission spectra

Fluorescence emission spectra were obtained using a Cary Eclipse spectrofluorometer, with both excitation and emission slits calibrated to 5 nm. Measurements were taken at 0.5 nm intervals, averaging over a 0.5 s duration. The excitation was consistently set at 280 nm, and the spectral analysis spanned from 250–550 nm. To account for inner filter effects and ensure accurate quenching results, corrections were applied using the formula: $F_{corr} = F_{obs} \times 10^{[(A_{exc}+A_{em})/2]}$, where F_{corr} and F_{obs} denote the corrected and observed fluorescence intensities, respectively. A_{exc} and A_{em} represent the system's absorptions at the excitation and emission wavelengths, respectively. Data analysis was facilitated by the UV-Vis-IR Spectral Software (FluorTools) [34]. The fluorescence spectra of the Ovalbumin-catanionic compound complexes were examined in a manner analogous to the UV-vis approach. Initially, each ligand was added individually, followed by the combined catanionic mixture. Concentrations for these measurements varied between 0.083 mM and 0.83 mM.

2.2.4. Circular Dichroism (CD)

Utilizing a JASCO-715 spectropolarimeter (Japan) equipped with a JASCO PTC-343 Peltier-regulated cell holder, Far-UV circular dichroism (CD) spectra were procured. For spectral acquisition, quartz cuvettes possessing a pathlength of precisely 0.2 cm were employed. The spectral range was recorder between 190 and 280 nm for both pure protein and ligand solutions. The protein sample was 1 mg/mL, corresponding to a molarity of 0.02 mM. Concurrently, a mixture of dicloxacillin and CTAB was added, with concentrations ranged from 0.83 to 4.2 mM for both compounds. Instrumental parameters were meticulously set: a resolution and bandwidth both at 1 nm, sensitivity calibrated at 50 mdeg, a response interval of 8 s, an accumulation factor of 3, and a scanning velocity of 50 nm/min. Any absorbance attributable to doubly distilled water was methodically negated, adhering to the instrumental parameters. Experimental data were expressed in terms of molar ellipticity by the equation $[\theta]_\lambda = \theta_\lambda M_r/ncl$, where M_r is the molecular weight of the protein, n represents residue quantity, c is the protein concentration, l corresponds to the cuvette's path length, and θ_λ is the ellipticity at a wavelength λ given by the apparatus. The resultant CD profiles represent the composite spectra inherent to α-helix, β-sheet, β-turn, and random coil configurations. Subsequent analysis of secondary structure composition was conducted using the webserver BeStSel software [35].

3. Results and discussion

3.1 Computational approaches

3.1.1 Binding site prediction and structural characterization

Predicting binding sites is generally a complex and challenging task, with different strategies and methods being suitable depending on the specific target molecule and applications. In this context, we used the ezPocket tool to computationally predict and identify potential binding sites on the ovalbumin as receptor, which resulted in ten potential binding pockets spread across the ovalbumin's surface. To this end, the ezPocket tool was applied which has been systematically used and validated in the context of multiple modeling problems [28, 36]. It works by identifying concave cavities that could potentially bind ligands (such as CTAB and dicloxacillin) and excluding convex ones in the protein structure, considering the ovalbumin's shape and size, as shown in **Figure 1**.

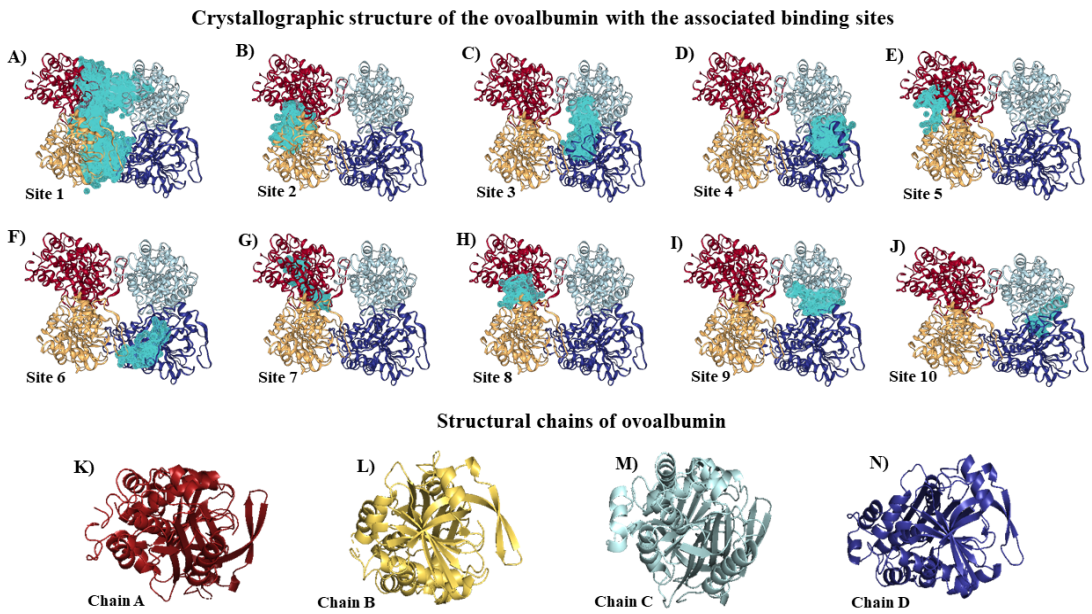

Figure 1. On the top, from panel **A)** to panel **J)**, is depicted the whole crystallographic 3D-structure of the ovalbumin with the predicted binding sites (from site θ =1 to θ =10) spread across the ovalbumin's surface as van der Waals volumetric surface labelled-cyan. In the bottom is represented a breakdown of the four ovalbumin's constitutional chains as **K)** chain A (labelled-red), **L)** chain B (labelled-yellow), **M)** chain C (labelled-light blue), and **N)** chain D (labelled-dark blue).

The **Figure 1** results on the binding sites prediction allow us to understanding the topological characteristics and size of the binding pockets in the ovalbumin which is crucial for understanding both, its function, and potential applications in structure-based drug design. Herein, the identified binding sites and their intrinsic structural differences (i.e., the constitutional chains A, B, C, D determining the pocket dimensions Vol($Å^3$) (please, refer to **Materials and methods section 2.1.1**) will further determine the stability-based binding affinity, type and strengths of interactions with the evaluated molecules (CTAB and dicloxacillin) will bind and undergo a chemical reaction under mixture combination [28, 36]. These sites are typically pockets or grooves on the ovalbumin's surface that could fit the physiological substrates both in shape and in the chemical characteristics and could be directly affected by the interaction of the ligands dicloxacillin and CTAB by separated, or by the interaction with the mixture (i.e., CTAB plus dicloxacillin). Then, knowing the properties of these ten predicted binding sites (from site 1 to site 10) associated with the cited structural chains that form part of each of them, allows us to understand the ligand specificity by the ovalbumin protein, its binding mechanism, and theoretically explain potential binding perturbations which will be addressed in detail in the following sections.

In the binding mixture scenario, the study of docking interactions of ligands (as CTAB plus dicloxacillin) holds significant relevance. Then, CTAB and dicloxacillin could act by interacting with the binding sites of the ovalbumin, either amplifying or inhibiting the protein's activity. The combination of CTAB and dicloxacillin could interact with the active sites in unique ways, potentially leading to a range of effects. This could result in synergistic binding effects, where the combined impact of the CTAB and dicloxacillin ligands is greater than the sum of their individual effects. Alternatively, it could lead to antagonism or competitive inhibition, where the cited mixture of ligands competes for the same binding site in the ovalbumin. Further explanation will be provided later.

3.1.2 Computational modelling on the mixture binding affinity

In the following discussion, we will examine the relationship between key factors to theoretically elucidate the effect of the mixture on its interaction with ovalbumin. We have employed several approaches to achieve this, including: i) assessing the thermodynamic binding affinity (ΔG, kcal/mol) in relation to the frequency of binding, ii) constructing a comprehensive isobologram combination index (CI) heatmap to understand the binding mechanism of the mixture as either antagonistic or synergistic, with theoretical concentrations obtained after docking simulation, and iii) conducting a site-specific and global evaluation of the fractional binding occupancy in relation to the combination index of the mixture. Please refer to **Figure 2** for a visual representation.

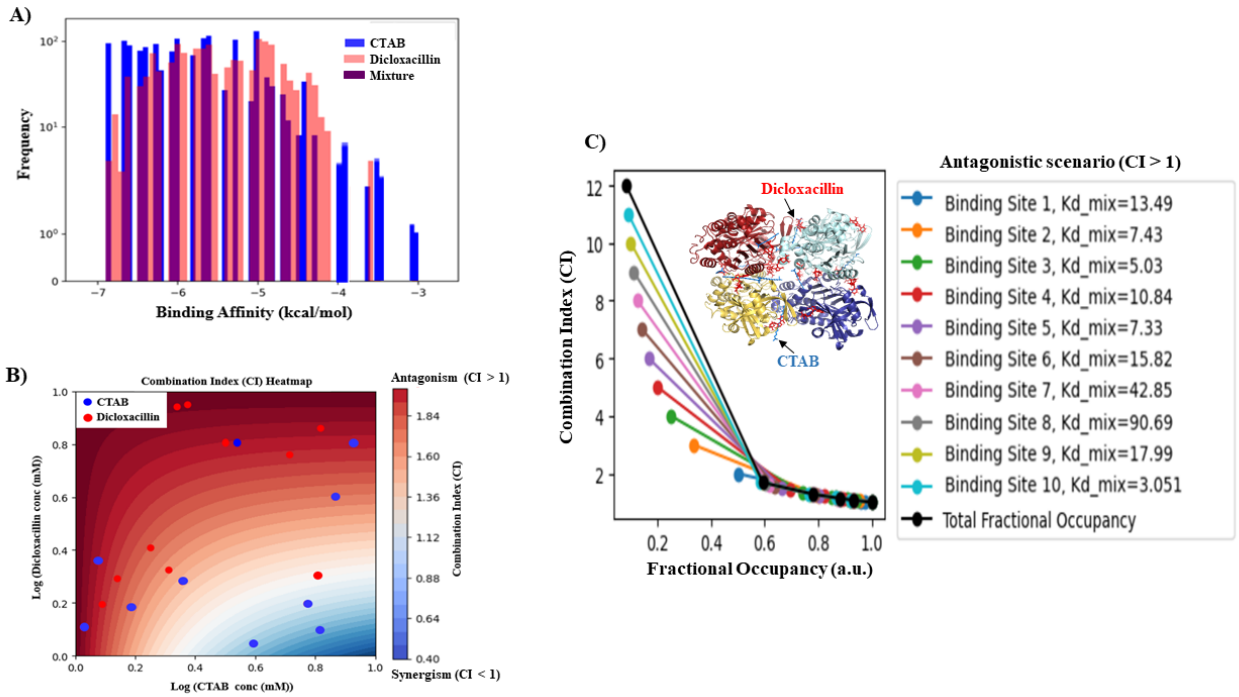

Figure 2. A) Graphical representation of the overall docking results showing the relationship between the binding affinity ΔG (kcal/mol) vs. frequency of binding by considering the three main ligand interaction evaluated in this study as CTAB (labelled-blue bars), dicloxacillin (labelled-pink bars), and the mixture CTAB plus dicloxacillin (labelled-dark red bars) for the whole structure of ovalbumin. **B)** Graphical representation of the theoretical 2D-isobolograms between CTAB and dicloxacillin under mixture binding combination in the whole lysozyme. Herein, the intensity bar color in the right-side of the heatmap is to represent the combination index (CI) of the evaluated mixture where labeled-red region ($CI_{(CTAB\text{-}Dicloxacillin)}$ > 1) corresponds to antagonistic binding effects. While labeled-blue region ($CI_{(CTAB\text{-}Dicloxacillin)}$ < 1) corresponds to synergistic binding effects, red and blue circles scattered in the heatmap represent the different conformations for both ligand CTAB and dicloxacillin; respectively. **C)** Graphical representation of the relationship between the fractional occupancy vs. combination index of the mixture in an antagonism scenario (CI > 1) showing a decrease in antagonistic behavior (CI > 1) with increasing fractional occupancy for individual site-specific and global interactions with the protein. Also, the values for the dissociation constants of the mixture (Kd_mix) in each binding site (θ; form the site θ =1 to θ =10) are represented.

First, we will begin by examining the thermodynamic binding affinity results to gain an understanding of the interaction strength between the ligands (CTAB and dicloxacillin) and the active sites of ovalbumin. A lower ΔG value (kcal/mol) indicates a more favourable interaction, which can be linked to a higher frequency of binding. Regarding the **Figure 2** panel **A)**, we can note that the ΔG affinity values of the CTAB and dicloxacillin mixture range from -6.9 kcal/mol to -4.4 kcal/mol. It's also noticeable that the binding frequency of CTAB is two times higher (10^2) than the binding frequency (10)

of the dicloxacillin within the same affinity range. However, theoretically, the strength of the interactions for CTAB appear to be lower compared to dicloxacillin, based on the lowest binding affinity value of CTAB (ΔG = -3 kcal/mol) compared with the lowest affinity observed for dicloxacillin (ΔG = -3.7 kcal/mol). This suggests that while CTAB may bind more often with the ovalbumin binding sites, the interactions it forms are less energetically favourable compared to those formed by dicloxacillin.

This differential binding behaviour could have significant implications for the function of the ovalbumin protein. Because proteins work by binding to their physiological substrates at their active sites and facilitating biochemical reactions, the strength of this binding, as indicated by the binding affinity, could theoretically influence the rate and efficiency of these biochemical reactions and the overall function of the ovalbumin protein. Secondly, from the mechanistic point of view, the isobologram combination index (CI) heatmap allows us to visualize the binding mechanism of the CTAB plus dicloxacillin mixture [20, 22-26]. By examining the heatmap, we can determine whether the evaluated ligands in the mixture bind to the ovalbumin protein in a synergistic or antagonistic manner. Besides, the binding affinity observed in the interaction between the CTAB and dicloxacillin mixture with ovalbumin could be significantly influenced by several factors. These include: i) the obtained theoretical concentration range of the CTAB and dicloxacillin mixture being evaluated, ii) the combination index (CI) of the mixture, and iii) the unique amino-acid chain composition and molecular structure of the different ovalbumin binding pockets evaluated (refer to **Figure 1**). It's conceivable that mechanisms based on synergistic binding effects could coexist with antagonistic binding effects within the same ovalbumin pocket [20, 22-26]. This can be effectively studied by determining the CI by performing the whole isobologram considering that it includes all the binding pockets (i.e., covering form the site $\theta = 1$ to $\theta = 10$). See **Figure 2** panel **B)**.

For this instance, we could theoretically suggest the presence of both binding behaviours (i.e., antagonistic > synergistic ~ additive binding effect) for the catanionic mixture interacting with the protein. As shown in **Figure 2B**, the red-labelled region of the isobologram with CI (CTAB-dicloxacillin) > 1 represents antagonistic binding effects while the blue-labelled one with CI (CTAB-dicloxacillin) < 1 represents synergistic binding effects. Then, it is clear a predominance of antagonistic binding effects for the whole protein in the range of theoretical concentration from 0.1 mM to 1 mM for dicloxacillin and from 0.1 mM to 0.25 mM for the CTAB. Regarding the tendency to induce synergistic binding for the case of dicloxacillin appears in the range of theoretical

405 docking concentration from 0.1 mM to 0.2 mM while in the case of CTAB appears in the
406 concentration interval from 0.4 mM to 1 mM. The additive effects (CI = 1) seem to have
407 less relevance in the context of this study.
408 Lastly, the evaluation of the fractional binding occupancy in relation to the combination
409 index of the mixture provides a comprehensive view of how the ligands in the mixture
410 interact with the protein's active sites. This could help to understand how the mixture as
411 a whole system affects the function of the ovalbumin protein [37, 38].
412 According to the results obtained in the **Figure 2C**. In the context of the relationship
413 between the fractional occupancy vs. combination index (CI) graph, a global and
414 individual decrease within an antagonistic scenario (CI > 1). Could increase the fractional
415 occupancy as showed. This fact suggests that, as more binding sites on the ovalbumin are
416 occupied by the ligands in the mixture, the overall interaction becomes less antagonistic.
417 This could be attributed to various factors, such as changes in the binding site
418 conformation or the influence of different CTAB and/or dicloxacillin binding
419 conformations linked to alterations in the local biophysical environment at the binding
420 sites [37, 38].
421 From a biochemical perspective, this shift from antagonism to less antagonistic or even
422 potentially synergistic interactions could have significant implications. It could alter the
423 rate and efficiency of the reactions catalysed by the ovalbumin protein, potentially
424 affecting catalytic pathways in which ovalbumin is involved. Regarding the dissociation
425 constants of the mixture (as Kd_mix) in each binding site of the ovalbumin provided
426 valuable insights into the binding affinities of the CTAB and dicloxacillin mixture with
427 ovalbumin. Lower Kd values indicate stronger binding affinities, suggesting that binding
428 sites 3 and 10 have the strongest interactions with the mixture, while binding sites 8 and
429 7 have the weakest. This differential binding affinity could theoretically could modules
430 the activity of the ovalbumin when separately evaluated [37-40].
431

432 ***3.1.3 Results on conformational drug-drug interaction network on ovalbumin***

433 In the context of this mechanistic study, it is essential to address not only the drug-drug
434 interactions within the entire mixture formed by the CTAB and dicloxacillin system but
435 also interactions that may occur individually, such as CTAB with CTAB or dicloxacillin
436 with dicloxacillin in a drug-drug interaction system. The complexity of the issue

intensifies when we simulate the influence of various conformations interacting with different binding sites of the protein [41-44].

Understanding the conformational drug-drug interaction network requires us to consider the intricate interplay between different ligands within the mixture and how these interactions could vary depending on the specific binding sites on the ovalbumin protein. This comprehensive exploration is essential to understand the interdependent conformational network of synergistic or antagonistic effects on the structure, dynamics, and interactions of ovalbumin, which may have significant implications for its biochemical function. To address the high-dimensionality of this conformational network problem, mechanistic results and corresponding interpretations will be provided for both the best- and worst-ranked binding sites of ovalbumin based on the stability of the formed docking complexes. See **Figure 3.**

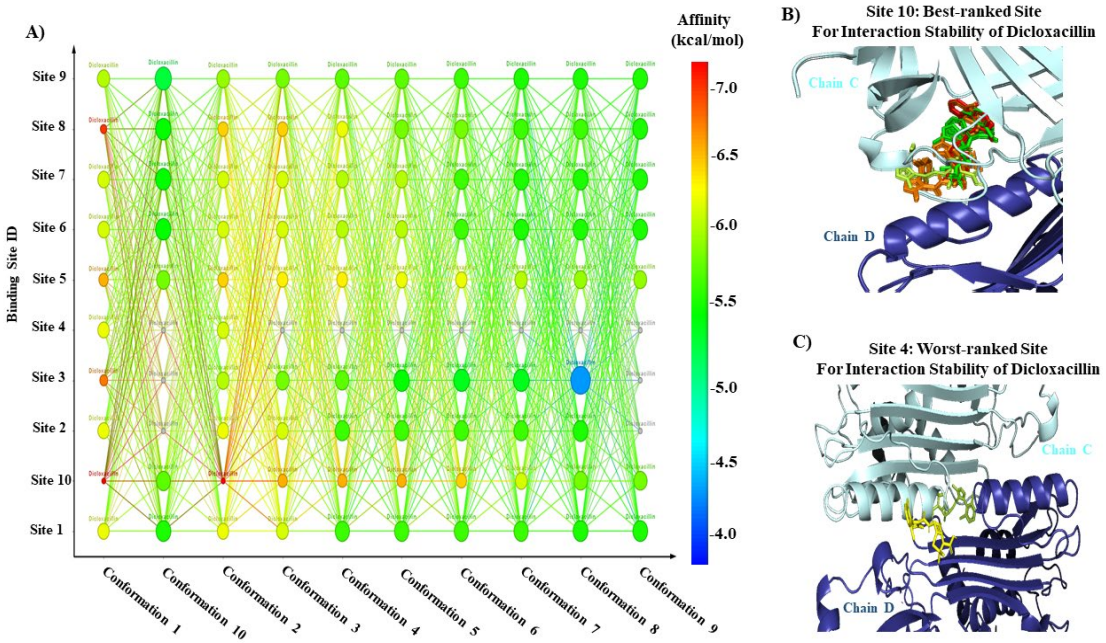

Figure 3. A) Representation of the conformational drug-drug interaction network within the same category (dicloxacillin plus dicloxacillin) showing the conformational network architecture resulting from the docking interactions with the different binding sites of the ovalbumin (covering form the site $\theta = 1$ to $\theta = 10$). Herein, the associated colour intensity bar (from blue to red) in the right-side of the network is to represents the strength of the interactions-based affinity (kcal/mol). Being the x-axis the i-conformation (dicloxacillin) vs. the y-axis as the specific j-binding site evaluated. **B)** Representation of the best-ranked binding site of the ovalbumin (site 10, chains C and D) showing the best interaction stability of the docking complexes for the dicloxacillin plus dicloxacillin system (network nodes mainly labelled-yellow to red). **C)** Representation of the worst-ranked binding site of the ovalbumin (site 4, chains C and D) showing the worst interaction stability of the docking complexes for the dicloxacillin plus dicloxacillin system (network

nodes mainly labelled-grey to light green) that means lower docking stability in the binding site 4 (just two dicloxacillin poses were detected).

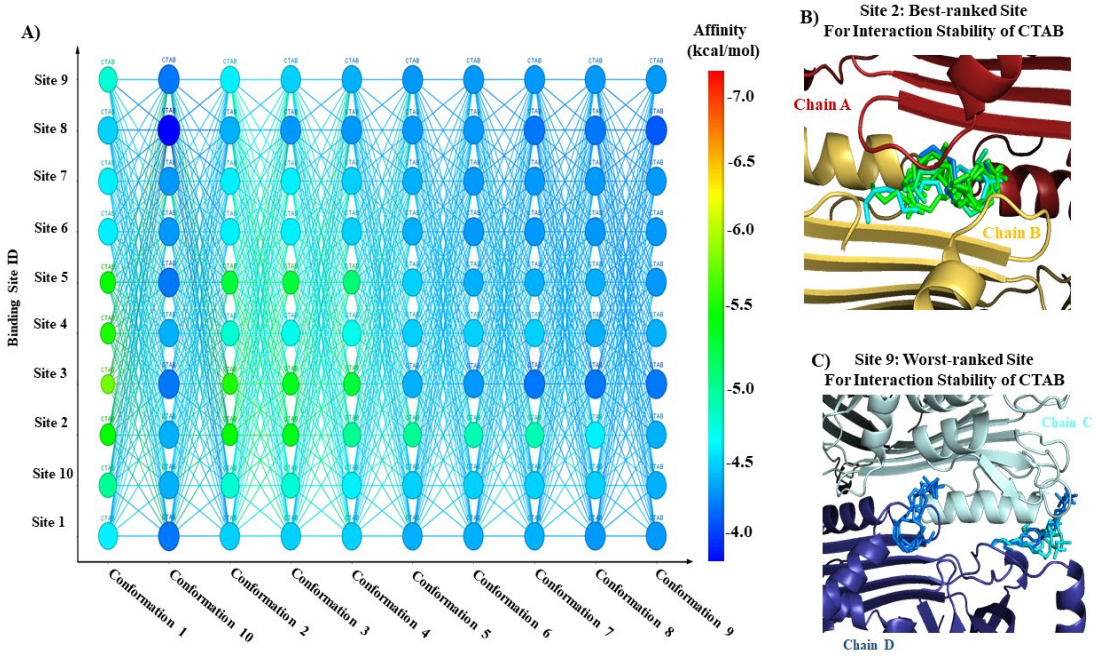

Figure 4. A) Representation of the conformational drug-drug interaction network within the same category (CTAB plus CTAB) showing the conformational network architecture resulting from the docking interactions with the different binding sites of the ovalbumin (covering form the site θ =1 to θ =10). Herein, the associated colour intensity bar (from blue to red) in the right-side of the network is to represents the strength of the interactions-based affinity (kcal/mol). Being the x-axis the i-conformation (CTAB) vs. the y-axis as the specific j-binding site evaluated. **B)** Representation of the best-ranked binding site of the ovalbumin (site 2, chains A and B) showing the best interaction stability of the docking complexes for the CTAB plus CTAB system (network nodes mainly labelled-blue to green). **C)** Representation of the worst-ranked binding site of the ovalbumin (site 9, chains C and D) showing the worst interaction stability of the docking complexes for the CTAB plus CTAB system (network nodes mainly labelled light blue to dark blue) that means lower docking stability in the binding site 9 (just four CTAB poses were detected).

In both drug-drug interaction networks, involving the same category as i) dicloxacillin plus dicloxacillin and ii) CTAB plus CTAB, a mechanistic and molecular docking analysis was performed to elucidate their conformational architectures within the context of different ovalbumin binding sites. The obtained conformational networks allow us to illustrate the conformational landscape resulting from docking interaction affinity across the different binding sites evaluated (θ = 1 to θ = 10). In the dicloxacillin system, the best-ranked binding site (site 10) exhibited high interaction stability, indicated by predominantly yellow to red network nodes, while the worst-ranked binding site (site 4)

displayed lower stability, shown as primarily grey to light green nodes. Similarly, in the CTAB system, the best-ranked binding site (site 2) demonstrated strong interaction stability (blue to green nodes), whereas the worst-ranked binding site (site 9) exhibited lower stability, shown with light blue to dark blue nodes.

Regarding the two conformational drug-drug interaction networks obtained for the isolated systems (i.e., pure or without the mixture) represented by as: i) conformational network of dicloxacillin-dicloxacillin interaction (**Figure 3A**) and ii) conformational network of CTAB-CTAB interaction (**Figure 4A**). It is clear to note that, the obtained values of the interaction affinity (kcal/mol) for the conformational dicloxacillin-dicloxacillin network interacting system exhibits significantly higher affinity values (in the range from -5.5 kcal/mol to -7.0 kcal/mol) compared with the conformational CTAB-CTAB network interacting systems (in the range from -4.0 kcal/mol to -5.0 kcal/mol). This theoretical insight is strongly associated with a higher strength of interactions for dicloxacillin-dicloxacillin drug-drug system respect to the CTAB-CTAB which was expressed in overall ovalbumin binding site evaluated. It is well-known that, from a thermodynamic-based interaction stability point of view, a more negative values of the Gibbs free energy ΔG (kcal/mol) indicates the formation of more stable docking complexes (i.e., dicloxacillin-dicloxacillin plus OVA >> CTAB-CTAB plus OVA). Except for the network nodes dicloxacillin-dicloxacillin which include the conformations 3, 4, 5, 6, 8 and 10 of the dicloxacillin-dicloxacillin drug-drug system placed within the binding site $\theta = 4$, where energetically unfavorable dicloxacillin-dicloxacillin plus OVA docking complexes were obtained. Suggesting either an extremely low or complete absence of binding affinity maybe by the presence of repulsive interactions in this specific biophysical environment ($\theta = 4$) nodes-labelled as gray).

The consideration of drug-drug interactions within the same category (i.e., CTAB plus CTAB and dicloxacillin plus dicloxacillin) is an imperative to discern how these interactions may contribute independently to the overall conformational landscape of the ovalbumin protein. The conformational drug-drug interaction network under investigation not only involves the interactions within the mixture but also the study of interactions occurring individually. The simultaneous exploration of these aspects provides a more comprehensive understanding of the intricate mechanisms at play, particularly when considering the diverse conformations interacting with various binding sites of the ovalbumin. These theoretical findings collectively emphasize the significance of understanding the specific binding sites and their corresponding interaction stabilities

alone as a starting point to understand the conformational binding of the mixture as showed in the **Figure 5**.

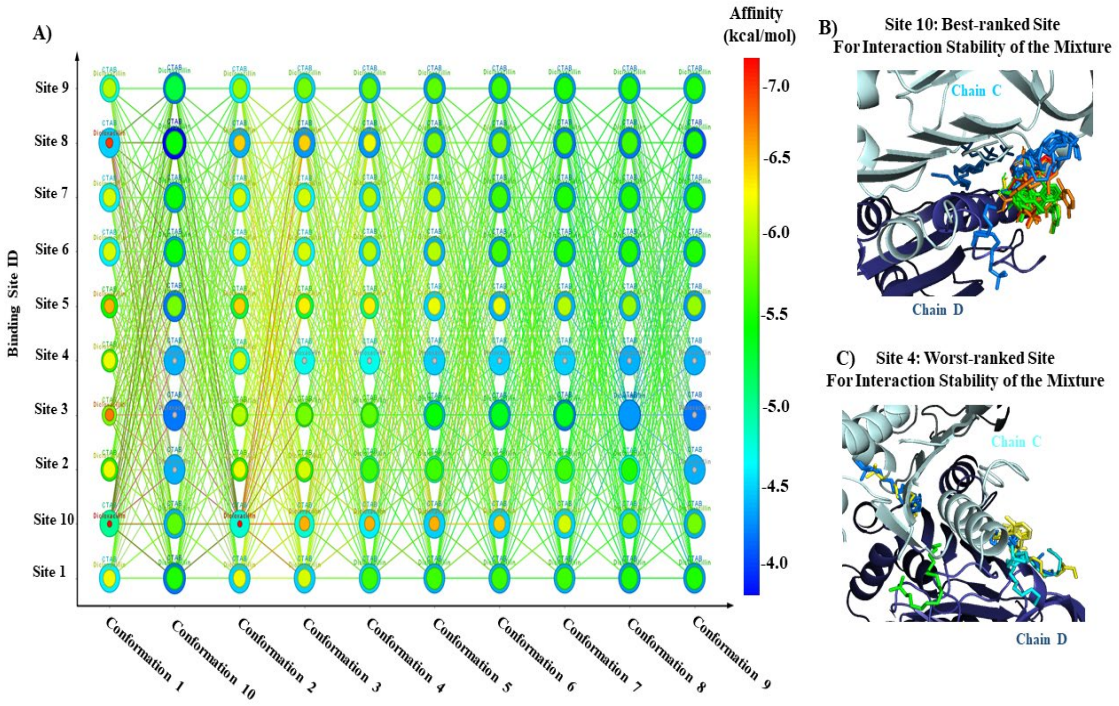

Figure 5. A) Representation of the conformational drug-drug interaction network for the mixture formed by dicloxacillin and CTAB showing the conformational network architecture resulting from the mixture with the different binding sites of the ovalbumin (covering form the site θ =1 to θ =10). Herein, the associated colour intensity bar (from blue to red) in the right-side of the network is to represents the strength of the interactions-based affinity (kcal/mol) of the mixture. Being the x-axis the i-conformation (dicloxacillin + CTAB) vs. the y-axis as the specific j-binding site evaluated. **B)** Representation of the best-ranked binding site of the ovalbumin (site 10, chains C and D) showing the best interaction stability of the docking complexes coming from the mixture dicloxacillin plus dicloxacillin (network mixed nodes mainly labelled-mixed orange + green to green + blue colour). **C)** Representation of the worst-ranked binding site of the ovalbumin (site 4, chains C and D) showing the worst interaction stability of the docking complexes for the dicloxacillin plus dicloxacillin system (network mixed nodes mainly labelled mixed blue + grey) that means lower docking stability for the mixture in the binding site 4.

In order to provide an integrated discussion on the mechanistic implications of our conformational drug-drug interaction network results, we focus solely on the top-ranked and lowest-ranked binding sites of ovalbumin. This involves considering the stability of the formed docking complexes with the ligand surfactants acting individually and forming the mixture in three representative drug-drug binding scenarios: i) OVA + dicloxacillin, ii) OVA + CTAB, and iii) the mixtures of OVA + dicloxacillin plus CTAB. In this context, for all the binding scenarios, was theoretically observed that, for the top-ranked binding sites (**Figure 3B**, **Figure 4B**, and **Figure 5B**), the ligands can interact

strongly and simultaneously in the same biophysical environment with the corresponding best-ranked binding sites identified. Specifically, in the case of dicloxacillin drug-drug interactions (see Figure 3B) with the binding site 10 formed between the β-sheets of chain C and the α-helix from chain D. In the case of CTAB, drug-drug interactions occur specifically within binding site 2 formed by two β-loops from a β-sheet and an α-helix that belong to chains A and B, respectively (see **Figure 4B**). On the other hand, in the case of the mixture dicloxacillin plus CTAB, the best-ranked binding site was found in site 10. For this instance, the target pocket is formed by a β-sheet and α-helix from chains C and D, respectively (**Figure 5B**). The theoretical evidence obtained for the best-ranked binding sites strongly suggests that the influence of the mixture (dicloxacillin + CTAB) could have a higher impact than the ligands (dicloxacillin and CTAB) acting separately (please refer to **equation 1**). In this context, from a mechanistic point of view, the occurrence of binding antagonistic mechanisms (CI > 1) is more likely than the occurrence of synergistic binding effects (CI < 1) due to the different physicochemical nature of the evaluated ligands and the simultaneous interaction of ligands in the same biophysical environment, which could also be modulated by the influence of steric factors under mixture interaction.

On the other hand, when analyzing the binding scenario based on the worst-ranked binding sites in the obtained docking complexes with ovalbumin (**Figure 3C**, **Figure 4C**, and **Figure 5C**), we can corroborate that the number of ligand molecules that can bind to these low-affinity sites is significantly lower compared to the best-ranked binding sites cited above. Besides, it is possible to observe that the distribution of ligand molecules is not only restricted to the same biophysical environment as in the previous case (with the best-ranked stability sites for docking), but also the binding distribution was found to be more randomly localized in the ovalbumin binding site structure. This fact suggests that the interaction of individual molecules could occur more likely than the interaction of the mixture (dicloxacillin plus CTAB) for the predicted worst-ranked binding sites (site 4, site 9 involving the chains C and D). In these cases, we could theoretically expect that the combination index (CI) is not affected by the influence of the dicloxacillin + CTAB mixture concentration. However, it could be influenced by the concentration of the ligands acting separately, which is frequently associated with potential synergistic (CI < 1) or additive effects (CI = 1) (please refer to **Figure 2B** above on the combination index CI). Many other relevant factors could affect the biochemical function of ovalbumin in both the unbound and bound states, such as structural perturbations linked to

574 conformational changes that influence the flexibility profile of the ovalbumin protein
575 induced by the ligands and their mixture. Further details can be found in the
576 supplementary information (**Figure S1**).
577 The exploration of the conformational drug-drug interaction network for the entire
578 mixture of dicloxacillin and CTAB is of significant importance in elucidating the
579 antagonist binding obtained above [41-44]. This multimodal approach provides a detailed
580 picture of how the mixture interacts with different binding sites on ovalbumin,
581 showcasing variable stability across these binding sites. Understanding the intricacies of
582 these interactions could shed light on the dynamics of mixture binding. Such theoretical
583 insights not only contribute to our comprehension of the molecular interplay within the
584 mixture but also offer valuable information for the design and optimization of better
585 therapeutic strategies where antagonistic interactions play a crucial role. Therefore, the
586 conformational drug-drug interaction network emerges as a powerful tool for dissecting
587 the complex landscape of antagonist binding in the studied mixture [41-44].
588
589 ***3.2. Experimental validation***
590 ***3.2.1. Absorbance Changes in Ovalbumin Analysis***
591 By leveraging computational simulations, we gain a molecular-level understanding
592 of the interactions within the system, predicting potential binding sites and energy
593 landscapes. These theoretical insights guide our experimental design, providing a
594 roadmap for targeted analyses. Subsequently, experimental findings validate and refine
595 the computational predictions, establishing a reciprocal relationship between theory and
596 practice. To this end, we analyzed absorbance shifts in ovalbumin, which are key to
597 unraveling interaction dynamics. Ovalbumin's UV-Vis absorbance spectrum is
598 intrinsically linked to the presence of its aromatic amino acid residues, primarily
599 tryptophan (Trp) and tyrosine (Tyr), which significantly contribute to its optical
600 properties. Tryptophan, with its complex indole ring structure, is particularly instrumental
601 in determining the protein's spectral behaviour. The indole ring's extensive conjugation
602 allows it to efficiently absorb light in the ultraviolet region, resulting in a dominant
603 absorbance peak at approximately 280 nm, **Figure 6**. This peak is primarily driven by
604 $\pi \rightarrow \pi^*$ electronic transitions within the indole ring. Tyrosine, with its phenolic ring
605 structure, adds to the UV-Vis absorbance spectrum of ovalbumin, typically manifesting
606 with peaks in the range of 270-275 nm. While less intense compared to tryptophan, these
607 tyrosine-associated peaks are nevertheless vital for the overall spectral profile. The

608 absorbance characteristics of these aromatic residues are sensitive to changes in the
609 protein's local environment, including alterations in pH, temperature, or interactions with
610 ligands. Therefore, a comprehensive understanding of ovalbumin's UV-Vis absorbance
611 properties, notably its aromatic amino acid residues, offers a crucial foundation for
612 studying its structural dynamics and the impact of various ligands on the protein's
613 absorbance spectrum. This insight is fundamental to elucidating the structural
614 transformations and binding interactions of ovalbumin and similar proteins in a variety
615 of applications. In the case of dicloxacillin, the UV-Vis absorbance primarily arises from
616 the presence of conjugated functional groups within its molecular structure, with distinct
617 features that reflect its electronic transitions. The absorbance spectrum of dicloxacillin
618 typically displays peaks at specific wavelengths, namely 274 and 280 nm, **Figure 6**,
619 indicative of the presence of chromophoric moieties, including aromatic rings and
620 carbonyl groups. These structural elements are prone to $\pi \rightarrow \pi^*$ and $n \rightarrow \pi^*$ electronic
621 transitions. For its part, the UV-Vis absorbance spectrum of CTAB exhibits main peaks
622 and absorption bands within the 200-300 nm range. Below the Critical Micelle
623 Concentration (CMC), peaks around 205 nm and 215 nm are observed, associated with
624 electronic transitions within individual CTAB molecules. Near the CMC, when CTAB
625 forms micelles, new peaks appear at longer wavelengths (around 250-300 nm), signifying
626 the collective behaviour of CTAB molecules within the micelles. The relationship
627 between concentration and absorbance becomes nonlinear above the CMC, with a
628 saturation effect, signifying the collective behaviour of surfactant molecules within the
629 micelles. This transition often results in a red shift, leading to the emergence of these
630 distinctive absorption peaks. In the present case, the highest value of the ovalbumin 278
631 nm band increases at 298 K upon complexation with the catanionic complex until
632 reaching a maximum value (**Figure 6A), curve ii.**)), then the maximum absorption
633 decreases regularly with increasing concentrations of the ligand mixture, indicating a
634 decrease in hydrophobicity and an increase in polarity [15]. Besides, the red shift
635 observed can be explained by the π-π stacking contact between the aromatic ring of the
636 dicloxacillin molecule and the phenyl rings of amino acid residues, combining charge
637 transfer and hydrophobic forces.

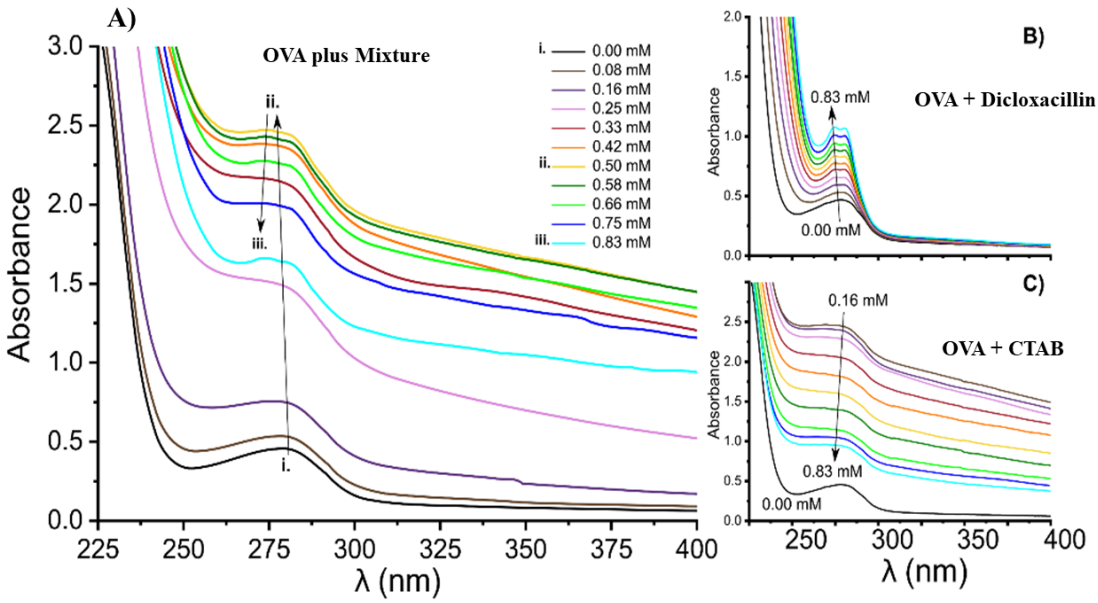

Figure 6. A) Absorbance spectra of OVA (C_{OVA} = 0.02 mM) in the absence (unbound OVA) and in the presence of the mixture of surfactant (Dicloxacillin plus CTAB). **B)** Absorbance spectra of increasing concentrations of Dicloxacillin. **C)** Absorbance spectra of increasing concentrations of CTAB. C_{Diclox} = C_{CTAB} as 0.08 mM, 0.16 mM, 0.25 mM, 0.33 mM, 0.42 mM, 0.50 mM, 0.58 mM, 0.66 mM, 0.75 mM, 0.83 mM.

3.2.2 Assessment of fluorescence features

The primary component of the OVA fluorescence spectrum is the Trp fluorescence. Specifically, OVA contains three Trp residues with distinct structural placements: Trp 160 is exposed to the solvent, Trp 194 is situated within a hydrophobic pocket, and Trp 275 is partially exposed. When varying amounts of ligands are added, a decrease in OVA fluorescence occurs within the 290-450 nm range, as depicted in **Figure 7**.

The stepwise addition of CTAB to the aqueous solution of the protein initially leads to a reduction in fluorescence intensity, a trend that persists until a value close to the critical micellar concentration of CTAB [45]. Subsequently, there is a gradual rise in fluorescence intensity until it reaches its maximum saturation level. Furthermore, it is worth noting that CTAB causes a blue shift in the fluorescence spectra once the probe-micelle interaction reaches saturation. In the lower concentration range of CTAB, the fluorescence intensity of ovalbumin notably decreases. This phenomenon is a common occurrence when dealing with lower surfactant concentrations and is often attributed to the formation of premicellar aggregates [45]. This effect is particularly pronounced with CTAB, given its long chain length [46]. Upon reaching a given concentration near the CMC, an enhancement in the emission yield becomes evident, indicating a marked

departure in the microenvironments enveloping these fluorophores within the CTAB medium in contrast to a pristine aqueous phase, occurrence already demonstrated by [45, 47].

It is well-documented that water can infiltrate micelles, reaching a certain depth that depends on the compactness of the micellar units [48]. Micelles characterized by more compact headgroups tend to experience less water penetration compared to micelles with less compact headgroups. Neutron scattering experiments conducted on micelles with varying surfactant chain lengths have revealed significant disparities in the headgroup structure of these micelles [48]. This observation strongly implies that as the surfactant chain length increases, the head-group becomes more compact. Consequently, water penetration is relatively minor in CTAB micelles when comparing with other bromide surfactants [45, 48]. Furthermore, the literature also reports an increase in the close packing and microviscosity of alkyltrimethylammonium bromide micelles as the alkyl chain length increases [49]. This leads to the fluorophore experiencing more rigid and less polar environments in CTAB micelles.

The observed shift towards the blue end of the spectrum in the fluorescence emissions upon the introduction of CTAB hints at the destabilization of the excited states of these complexes. It also signifies a decrease in the polarity of the micellar solution when compared to the aqueous medium. The fluorescent probe plays a central role in assessing the microscopic polarity of the bio-mimicking environment, utilizing diverse photo-physical parameters to offer a relative measure of the microenvironment's polarity. It's worth emphasizing that the polarities of homogeneous and micro-heterogeneous media cannot be presumed to be identical.

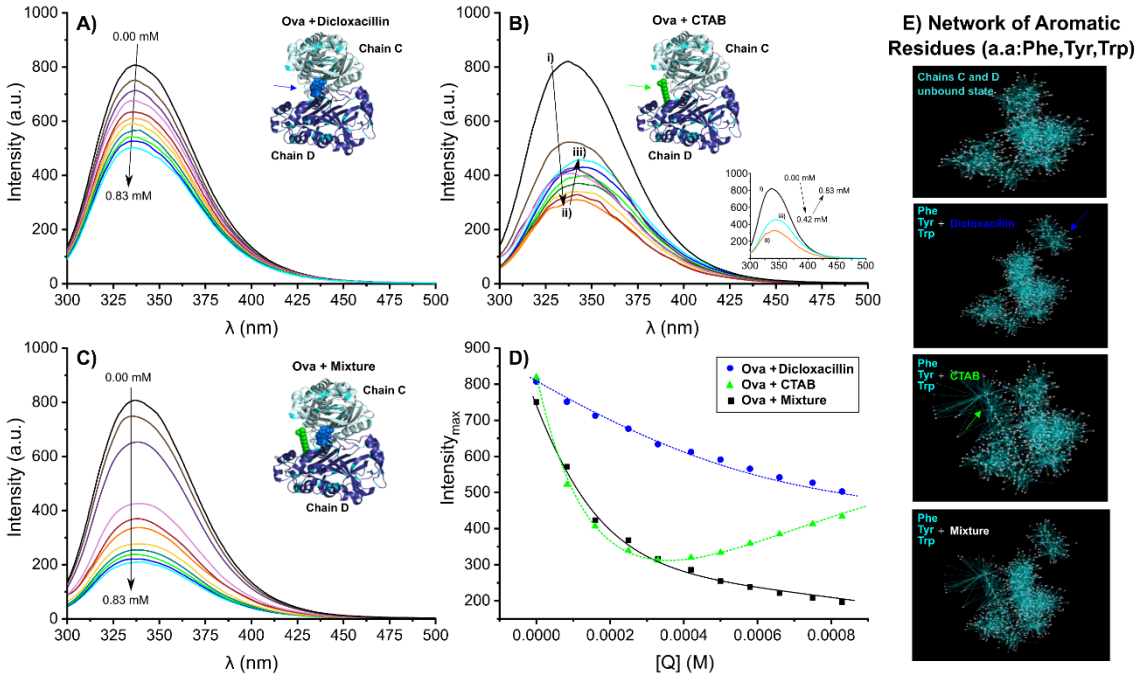

Figure 7. Fluorescence emission spectra obtained from the ovalbumin protein in different binding conditions as in the absence (Ova unbound state at 0.00 mM) and in the presence of the evaluated ligands as: **A)** Ova + dicloxacillin, **B)** Ova + CTAB, **C)** Ova + surfactant mixture (dicloxacillin + CTAB) and **D)** maximum intensity fluorescence vs. surfactant concentrations for the tree binding conditions evaluated (Ova + dicloxacillin, Ova + CTAB, Ova + surfactant mixture). **E)** Results on graph interaction networks of the fluorescence-sensitive aromatic residues (i.e., phenylalanine Phe, tyrosine Tyr, and tryptophan Trp) belonging to the ovalbumin target-chains (C and D) regarding the aforementioned binding conditions. Herein, ovalbumin = 0.02 mM, $C_{Dicloxacillin} = C_{CTAB}$ = (0.083 mM, 0.166 mM, 0.250 mM, 0.330 mM, 0.416 mM, 0.500 mM, 0.580 mM, 0.660 mM, 0.750 mM, 0.830 mM).

To assess the strength of the interaction between i) OVA and dicloxacillin, and ii) OVA and the mixture (i.e., CTAB + dicloxacillin), we performed fluorescence quenching for the tryptophan amino acid from OVA (OVA-Trp). The emission at 340 nm was analyzed using the Stern–Volmer analysis. In the context of the present study, the Stern-Volmer plot was used to evaluates the kinetics of the fluorescence deactivation (quenching of the OVA-Trp) induced by the ligands as dicloxacillin and the mixture CTAB + dicloxacillin (acting as the quenchers in both scenarios). In general, this process can be represented by the following simple equation: P* + Q → P + Q. Here, P* represents an excited state (denoted by "*") of the protein OVA-Trp, with fluorescence intensity (F) measured in the presence of a given ligand or quencher (Q). The resulting P represents a non-excited state of the protein OVA-Trp, with fluorescence intensity (F_0) measured in the absence of the quencher Q. The kinetics of this process follow the Stern-Volmer relationship, as described in **equation 2**.

$$\frac{F_0}{F} = 1 + K_{sv}[Q] \quad (2)$$

The parameter K_{sv} represents the Stern-Volmer quenching constant. By plotting the linear ratio of F_0/F versus the quencher's Q at different concentrations for each system (i.e., OVA plus dicloxacillin and OVA plus the mixture of CTAB + dicloxacillin), we can determine the experimental Stern-Volmer constant.

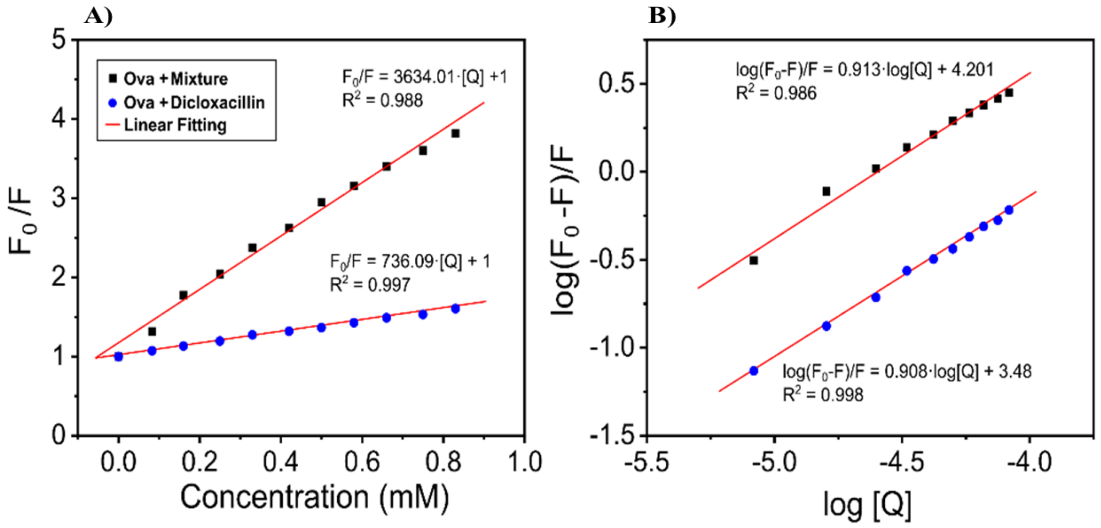

Figure 8. A) Stern-Volmer plots for the quenching of Ovalbumin by Diclox (○) and the mixture of surfactants (■). **B)** Plots of log[(F_0-F)/F] vs log[Q] of Diclox (○) and mixture of surfactants (■). $C_{Ovalbumin}$ = 0.02 mM.

As shown in the linear Stern-Volmer plot (**Figure 8A**), both ligand systems quench ovalbumin (OVA) fluorescence, allowing for the determination of the quenching rate constants and binding affinities. By applying the Stern - Volmer equation, we found that the quenching constants (K_{sv}) were 7.09 x 10^2 mol^{-1} and 33.78 x 10^2 mol^{-1} for the OVA plus dicloxacillin and OVA plus the mixture of CTAB + dicloxacillin); respectively. Assuming a Trp half-life of the emissive excited state of 10 ns in ovalbumin [50], the bimolecular quenching constant markedly exceeds the rate of diffusion-limited quenching, as in water, the maximum value of k_q for diffusion-limited quenching is approximately 10^{10} L mol^{-1} s^{-1} [51]. Consequently, we could infer the formation of stable complexes in solution for the evaluated systems by inducing the quenching of OVA fluorescence through a static mechanism. Next, the static fluorescence quenching mechanism allowed us to use **equation 3** to experimentally determine relevant binding parameters such as the Hill cooperativity binding coefficient (n) and the association constant (Ka) for the aforementioned systems.

$$log\frac{(F_0 - F)}{F} = logK_a + n \cdot log[Q] \quad (3)$$

In the **Figure 8B**, the obtained binding profile as two parallel lines in the plot of log [(F0 − F)/F] vs. log [Q] suggests a coherent relationship in the binding behavior of the evaluated systems, dicloxacillin and the CTAB plus dicloxacillin mixture, in terms of interaction with OVA binding sites. Since dicloxacillin is common in both interacting systems, the chemical properties of dicloxacillin may be the main responsible for the observed binding trend. In this regard, this quenching mechanisms (i.e., fluorescence decrease) could be indicative of the presence of potential antagonistic binding mechanisms in two different probable ways as: i) competition for OVA binding sites at the same biophysical environment as showed by the theoretical approaches (refer to **Figure 5B** and **Figure 7C**), ii) coexistence of uncompetitive and competitive inhibition, both of which are antagonistic and non-mutually exclusive mechanisms, involves network conformational changes influencing the binding affinity (refer to **Figure 5A**). Both mechanisms could independently modulate the quenching decrease of OVA interaction. However, additional studies, such as the application of a double reciprocal Lineweaver-Burk plot, could be proposed in future investigations of these hybrid mechanisms [52].

Next, The estimated binding parameters (n and Ka) for the aforementioned systems are presented in **Table 1**, following the application of **equation 3**. Regarding the obtained results derived from the **Figure 8B**, the slope (n) of the linear plot of log [(F_0 − F)/F] vs. log [Q] provides relevant information on the interaction behavior of the evaluated ligands-based quenchers (i.e., dicloxacillin and the mixture CTAB plus dicloxacillin) with the OVA binding sites. Here, the binding parameter 'n' corresponds to the experimentally obtained Hill cooperativity coefficient. The experimental parameter ‘n’ provides additional insights into the intrinsic dynamics of the OVA with the aforementioned interaction systems. This allows for a better explanation of the cooperativity behavior of binding, which could be associated with potential synergistic, additive, or antagonistic binding effects of the evaluated ligands with the OVA binding sites. Furthermore, there is widespread acknowledgment of the connection between the synergistic, additive, and antagonistic binding mechanisms with the Hill cooperativity binding coefficient (n) [53, 54]. From a rigorous mathematical perspective, the following expectations are associated with a mechanistic interpretation of the obtained Hill cooperativity binding coefficient (n) as: i) antagonistic binding manifests when the experimentally observed value of n is strictly < 1; ii) synergistic binding occurs when the value of n strictly > 1, and iii) an additive binding effect is anticipated when the value of n equals 1 [53, 54].Then, in

accordance with the docking results and the theoretical isobologram obtained (Please, refer to Figure 2B), the antagonistic effects seem to be predominant over synergistic effects in the concentration range from 0.4 mM to 1 mM.

By the other hand, the association binding constant (Ka) can be obtained from the intercept as Log Ka[53]. Here, the association constant (Ka) is a crucial parameter that allows for the measurement of the equilibrium constant for the binding association between the OVA and the evaluated ligand systems, providing a quantitative kinetic measure of the strength of the binding interaction. Therefore, a higher Ka value indicates a stronger binding affinity between the OVA protein and the ligands, such as dicloxacillin or the mixture of CTAB and dicloxacillin.

Table 1. Stern-Volmer quenching constants and binding parameters for the interaction of Ovalbumin with Dicloxacillin and the mixture CTAB plus dicloxacillin at 298 K.

Docking System ID	Stern-Volmer constants		Binding parameters		
	10^{-2} Ksv (mol^{-1})	R^2	n	10^3 K_a (mol^{-1})	R^2
OVA plus Diclox	7.09 ± 0.02	0.997	0.908 ± 0.01	3.02 ± 0.04	0.998
OVA plus Mixture	33.78 ± 0.05	0.989	0.913 ± 0.01	15.88 ± 0.01	0.986

In terms of the association constant, it is worth noting that the value for the mixture of CTAB + dicloxacillin is approximately 50 times higher than the value for dicloxacillin interacting alone. These results show that the drug's affinity for the OVA is relatively low but gets strengthened by the presence of CTAB in the mixture.

3.2.3 FRET Insights: Examining Molecular Bonds and Proximity

Energy transfer offers a more comprehensive insight into molecular interactions, and within the realm of investigating protein-ligand interactions and alterations in protein structure induced by ligand binding, Fluorescence Energy Transfer (FRET) is of paramount significance. FRET, firmly rooted in classical physics, operates as a non-invasive spectroscopic technique, facilitating the non-radioactive transfer of excitation energy from the protein ovalbumin, which functions as the donor molecule in this context, to the acceptor molecule(s) in their ground state. Donor molecules, in this scenario, typically emit photons at shorter wavelengths that significantly overlap with the absorption spectrum of the acceptor. In this specific case, the shifts observed in the fluorescence spectra of ovalbumin upon interaction with ligands reveal the occurrence of energy transfer between the ligands and the protein. Assessing the efficiency of energy transfer serves as a valuable means for estimating the proximity between the Trp residues

within the protein and the ligand. For energy transfer to exist, three essential criteria must be met: (1) the donor molecule should emit fluorescent light; (2) the absorption spectrum of the acceptor should exhibit substantial overlap with the fluorescence emission spectrum of the donor; and (3) the distance separating the donor and acceptor should be less than 8 - 10 nm [54]. As per Förster's theory, the efficiency of energy transfer (E) can be mathematically computed using the ensuing expression:

$$E = 1 - (F/F_0) = R_0^6/(R_0^6 + r^6) \quad (4)$$

F represents the fluorescence intensity exhibited by ovalbumin in the presence of ligands, whereas F0 signifies the intensity exhibited by the protein in isolation. The variable 'r' designates the distance at which binding occurs between the donor and the receptor, and 'R_0' denotes the critical distance for energy transfer. At 'R_0', precisely 50% of the excitation energy gets transferred to the acceptor. This particular parameter is ascertainable through the following mathematical expression:

$$R_0^6 = 8.79 \times 10^{-25}\, K^2\, n^{-4}\, \Phi\, J \quad (5)$$

In this context, K^2 stands for the spatial orientation factor between the dipoles of the donor and the acceptor, 'n' signifies the refractive index of the surrounding medium, Φ represents the fluorescence quantum yield of the donor (in this case, ovalbumin), and 'J' characterizes the spectral overlap between the emission spectrum of the donor and the absorption spectrum of the acceptor (in this case, dicloxacillin and CTAB). When determining 'R_0', the factor that introduces the most uncertainty is the dipole orientation factor, which can potentially vary from 0 to 4. However, in scenarios where both the protein and the ligands experience rapid tumbling and can assume any orientation, a commonly accepted value for K^2 is 2/3. The refractive index 'n' is typically assigned the value of 1.333, corresponding to the refractive index of water, while Φ is commonly assumed to be 0.15, aligning with the fluorescence quantum yield of tryptophan. Lastly, the spectral overlap can be computed as follows:

$$J = \frac{\int_0^\infty F(\lambda)\, \varepsilon(\lambda)\, \lambda^4\, \mathrm{d}\lambda}{\int_0^\infty F(\lambda)\, \mathrm{d}\lambda} \quad (6)$$

F(λ) is the fluorescence intensity of the protein and Ɛ(λ) is the molar absorption coefficient of the acceptor at a given wavelength λ.

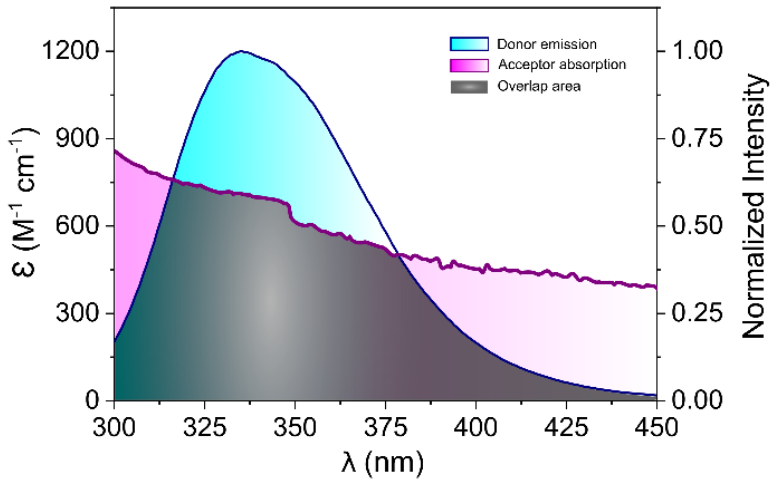

Figure 9. Overlap area (J(λ)) of donor fluorescence emission spectrum (blue) and acceptor absorption spectrum (purple). T = 298 K. C_{OVA} = 0.02 mM, C_{Diclox} = C_{CTAB} = 0.50 mM.

Following the explained methodology, **Figure 9** displays the overlap curves obtained, while **Table 2** provides the corresponding FRET values. Within the catanionic system, the binding distance (denoted as 'r') between the donor and receptor falls in the range of 2-8 nm. It is noteworthy that the conditions where 0.5 times 'R_0' is less than 'r' and 'r' is less than 1.5 times 'R_0' strongly indicate a high likelihood of energy transfer from ovalbumin to the ligands. This observation aligns with the presence of non-radiative energy transfer, signifying that the highly excited elements may return to the ground state [55]. Furthermore, these results provide additional support for the predominant involvement of static-type fluorescence mechanisms, as previously demonstrated.

Table 2. Fluorescence resonance energy transfer (FRET) results of the interaction between the protein Ovalbumin and the mixture of ligands.

Docking System ID	**FRET parameters**		
	J (M^{-1} cm^{-1} nm^4)	R_0 (Å)	r (nm)
OVA plus Mixture	7.98×10^{12}	18.85	2.59

3.2.4 Circular Dichroism (CD) Investigation: Probing Molecular Architecture and Structural Characteristics

Far-UV Circular Dichroism is a widely employed technique for discerning the α-helix and β-sheet secondary structural components in proteins, offering insights into their conformational variations. In this investigation, the influence of dicloxacillin and the mixture of surfactants on the secondary structure of ovalbumin was probed through far-UV CD spectroscopy. The outcomes revealed that the addition of varying concentrations of dicloxacillin, spanning from 0.083 to 0.33 mM, induced pronounced alterations in the

shape of the minima, accompanied by a notable decrease in negative ellipticity. These changes signify a reduction in the secondary structure of the protein. In a similar way, the mixture of both surfactants caused an even more pronounced alteration in the CD results (**Figure 10**).

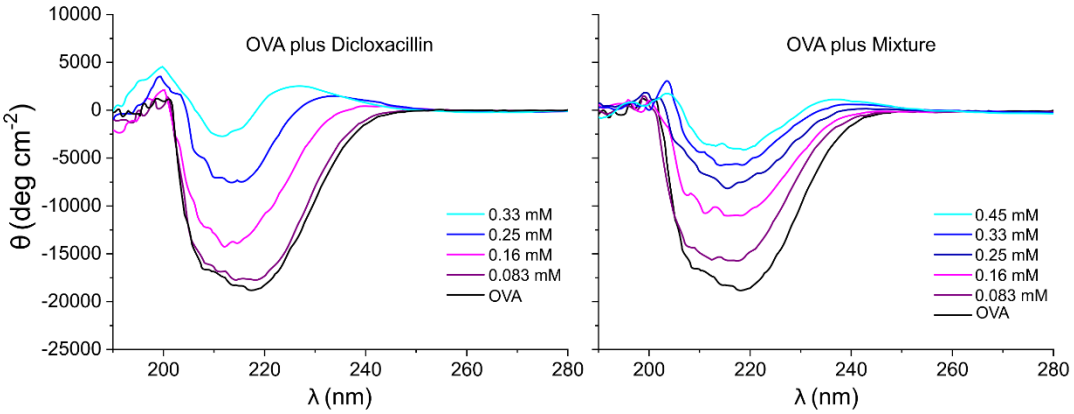

Figure 10. Far-UV CD spectra of OVA (C_{OVA} = 0.02 mM) with increasing concentrations of: **A)** OVA+ Dicloxacillin (C_{Diclox} = 0.083 mM, 0.16 mM, 0.25 mM, 0.33 mM) and **B)** OVA + Mixture (C_{Diclox} = C_{CTAB} = 0.083 mM, 0.16 mM, 0.25 mM, 0.33 mM, 0.45 mM).

To quantitatively assess these modifications, the BeStSel analysis was applied to compute the overall percentage of α-helix structural variations, and the results are outlined in **Table 3**.

Table 3. Quantitative results on the contents of ovalbumin α-helices elements (%) as a function of the surfactant mixture concentration added.

[Surfactant Mixture] (mM)	**α – Helix (%)**
0.0	38.24
0.083	32.51
0.16	30.98
0.25	28.75
0.33	27.01
0.42	25.13

As it can be inferred from the results, the mixture of dicloxacillin and CTAB can significantly influence the results obtained from circular dichroism (CD) spectroscopy when applied to ovalbumin. The cationic surfactant CTAB can bind to ovalbumin through electrostatic and hydrophobic interactions, disrupting the protein's native structure. Additionally, dicloxacillin, can also directly interact with ovalbumin, causing conformational shifts. These dual interactions may lead to synergistic effects or

competing influences on ovalbumin's secondary and tertiary structures, ultimately reflected in the CD spectra. The CD results show variations in the characteristic CD peaks associated with different secondary structural elements, such as α-helices and β-sheets, as well as in the near-UV region where changes in the local environment of aromatic residues are monitored. The chiral environment can also be altered due to these interactions, further impacting the CD spectra. Furthermore, any complex formation between ovalbumin, dicloxacillin, and CTAB will contribute to distinct CD signatures, possibly differing from those of individual components or unbound the protein. Therefore, a mixture of dicloxacillin and CTAB presents a complex interplay of structural modifications within ovalbumin, posing both cooperative and competitive effects that significantly influence the CD results and provide insights into the intricate interactions between the components of the mixture and the protein. It is important to note that mechanistic studies of interactions involving mixture of compounds still pose a significant challenge, and certain experimental limitations are inherent when increasing the complexity of the system under investigation. In this context, strategies for addressing these methodological issues are outlined in the supplementary material (**Table S1**).

4. Conclusions

Our research has combined computational modelling and experimental methods to enhance our comprehension of the intricate conformational binding between mixtures of dicloxacillin plus CTAB on the ovalbumin protein. This multi-modal network approach has led to significant advancements in our understanding of this subject matter. We identified active sites on ovalbumin and analysed the interaction dynamics, including the possibility of a prevalence of antagonistic binding effects over the synergistic and additive ones by using computational and spectrofluorimetric methods. Our thermodynamic analysis distinguished the isolated binding strengths of CTAB and dicloxacillin, revealing precise insights into their respective interactions with ovalbumin. These computational predictions were experimentally validated by observing changes in ovalbumin's fluorescence properties and confirmed by both, the Stern-Volmer analysis and circular dichroism spectroscopy. The findings fit excellent and confirmed the theoretical models emphasizing that mixture interactions could promote structural and conformational changes in whole ovalbumin and its relevant binding sites. Finally, by combining new computational approaches with experimentally validated spectrofluorimetric data, this work enhances the current understanding on the bio-interactions between proteins and

surfactant mixtures. The precise and efficient control over interfacial properties and the conformational behavior of ovalbumin during interaction with the isolated and mixed system could open new opportunities for applications in food processing, chemistry, and the rational design of pharmaceutical drugs.

Ethics approval and consent to participate

Not applicable.

Acknowledgements

M.G.D. thanks European Union's H2020 project Sinfonia (N.857253). R.R. and J.M.R. thank Xunta de Galicia for support (ED431B 2022/36). R.R. is granted by the Program for the requalification, international mobility, and attraction of talent in the Spanish university system, modality Margarita Salas (grant UP2021-042).

Author Contributions

Michael González-Durruthy: Conceptualization, Software, Methodology, Writing – original draft, Writing – review & editing. **Ramón Rial**: Conceptualization, Data curation, Formal analysis, Methodology, Writing – original draft, Writing – review & editing. **Juan M. Ruso**: Supervision, Conceptualization, Writing – review & editing.

References

[1] M. Aguirre-Ramírez, H. Silva-Jiménez, I.M. Banat, M.A. Díaz De Rienzo, Surfactants: physicochemical interactions with biological macromolecules, Biotechnology Letters 43(3) (2021) 523-535.

[2] M. Nikbakht Nasrabadi, A. Sedaghat Doost, R. Mezzenga, Modification approaches of plant-based proteins to improve their techno-functionality and use in food products, Food Hydrocolloids 118 (2021) 106789.

[3] J.M. Ruso, N. Deo, P. Somasundaran, Complexation between dodecyl sulfate surfactant and zein protein in solution, Langmuir 20(21) (2004) 8988-91.

[4] J. Maldonado-Valderrama, A. Martín-Molina, A. Martín-Rodriguez, M.A. Cabrerizo-Vílchez, M.J. Gálvez-Ruiz, D. Langevin, Surface Properties and Foam Stability of Protein/Surfactant Mixtures: Theory and Experiment, The Journal of Physical Chemistry C 111(6) (2007) 2715-2723.

[5] J. Maldonado-Valderrama, J.M.R. Patino, Interfacial rheology of protein–surfactant mixtures, Current Opinion in Colloid & Interface Science 15(4) (2010) 271-282.

[6] R. Miller, V.B. Fainerman, M.E. Leser, M. Michel, Surface tension of mixed non-ionic surfactant/protein solutions: comparison of a simple theoretical model with experiments, Colloids and Surfaces A: Physicochemical and Engineering Aspects 233(1) (2004) 39-42.

[7] C. Kotsmar, V. Pradines, V.S. Alahverdjieva, E.V. Aksenenko, V.B. Fainerman, V.I. Kovalchuk, J. Krägel, M.E. Leser, B.A. Noskov, R. Miller, Thermodynamics, adsorption kinetics and rheology of mixed protein–surfactant interfacial layers, Advances in Colloid and Interface Science 150(1) (2009) 41-54.

[8] A. Stenstam, A. Khan, H. Wennerström, Lysozyme in Catanionic Surfactant Mixtures, Langmuir 20(18) (2004) 7760-7765.

[9] J.X. Xiao, U. Sivars, F. Tjerneld, Phase behavior and protein partitioning in aqueous two-phase systems of cationic--anionic surfactant mixtures, Journal of chromatography. B, Biomedical sciences and applications 743(1-2) (2000) 327-38.

[10] E. Blanco, P. Messina, J.M. Ruso, G. Prieto, F. Sarmiento, Regarding the effect that different hydrocarbon/fluorocarbon surfactant mixtures have on their complexation with HSA, The journal of physical chemistry. B 110(23) (2006) 11369-76.

[11] L. Xu, L. Feng, S. Dong, J. Hao, Q. Yu, Carbon nanotubes modified by a paramagnetic cationic surfactant for migration of DNA and proteins, Colloids and Surfaces A: Physicochemical and Engineering Aspects 559 (2018) 201-208.

[12] F. Niu, F. Gu, M. Zhao, Y. Gao, W. Tu, M. Kou, W. Pan, Aggregation and Growth Mechanism of Ovalbumin and Sodium Carboxymethylcellulose Colloidal Particles under Thermal Induction, Biomacromolecules 24(3) (2023) 1532-1543.

[13] S.K. Davidson, D.A. Stahl, Selective recruitment of bacteria during embryogenesis of an earthworm, The ISME Journal 2(5) (2008) 510-518.

[14] X. Huang, Z. Tu, H. Wang, Q. Zhang, Y. Shi, H. Xiao, Increase of Ovalbumin Glycation by the Maillard Reaction after Disruption of the Disulfide Bridge Evaluated by Liquid Chromatography and High Resolution Mass Spectrometry, Journal of Agricultural and Food Chemistry 61(9) (2013) 2253-2262.

[15] Y. Zhao, Z. Chen, J. Li, M. Xu, Y. Shao, Y. Tu, Formation mechanism of ovalbumin gel induced by alkali, Food Hydrocolloids 61 (2016) 390-398.

[16] F. Niu, Q. Zhang, J. Yu, Y. Huo, L. Zhuo, D. Niu, W. Pan, Interfacial adsorption behavior of ovalbumin/ sodium carboxymethyl cellulose colloidal particles: The effects of preparation methods, Food Hydrocolloids 120 (2021) 106969.

[17] P. Taboada, D. Attwood, J.M. Ruso, M. García, F. Sarmiento, V. Mosquera, Influence of Molecular Structure on the Ideality of Mixing in Micelles Formed in Binary Mixtures of Surface-Active Drugs, Journal of Colloid and Interface Science 216(2) (1999) 270-275.

[18] P. Severino, M. Szymanski, M. Favaro, A.R. Azzoni, M.V. Chaud, M.H. Santana, A.M. Silva, E.B. Souto, Development and characterization of a cationic lipid nanocarrier as non-viral vector for gene therapy, European journal of pharmaceutical sciences : official journal of the European Federation for Pharmaceutical Sciences 66 (2015) 78-82.

[19] S. Ladame, Dynamic combinatorial chemistry: on the road to fulfilling the promise, Organic & Biomolecular Chemistry 6(2) (2008) 219-226.

[20] R. Rial, M. González-Durruthy, Z. Liu, J.M. Ruso, Conformational binding mechanism of lysozyme induced by interactions with penicillin antibiotic drugs, Journal of Molecular Liquids 358 (2022) 119081.

[21] Y. Liu, Z. Liu, G. Zeng, M. Chen, Y. Jiang, B. Shao, Z. Li, Y. Liu, Effect of surfactants on the interaction of phenol with laccase: Molecular docking and molecular dynamics simulation studies, Journal of Hazardous Materials 357 (2018) 10-18.

[22] T.C. Chou, Drug combination studies and their synergy quantification using the Chou-Talalay method, Cancer research 70(2) (2010) 440-6.

[23] F. Wong, A. Krishnan, E.J. Zheng, H. Stärk, A.L. Manson, A.M. Earl, T. Jaakkola, J.J. Collins, Benchmarking AlphaFold-enabled molecular docking predictions for antibiotic discovery, Molecular systems biology 18(9) (2022) e11081.

[24] D.J. Wooten, C.T. Meyer, A.L.R. Lubbock, V. Quaranta, C.F. Lopez, MuSyC is a consensus framework that unifies multi-drug synergy metrics for combinatorial drug discovery, Nature Communications 12(1) (2021) 4607.

[25] D.J. Wooten, R. Albert, synergy: a Python library for calculating, analyzing and visualizing drug combination synergy, Bioinformatics 37(10) (2020) 1473-1474.
[26] A. Ianevski, A.K. Giri, T. Aittokallio, SynergyFinder 2.0: visual analytics of multi-drug combination synergies, Nucleic Acids Research 48(W1) (2020) W488-W493.
[27] W.P. Feinstein, M. Brylinski, Calculating an optimal box size for ligand docking and virtual screening against experimental and predicted binding pockets, Journal of Cheminformatics 7(1) (2015) 18.
[28] V. Le Guilloux, P. Schmidtke, P. Tuffery, Fpocket: An open source platform for ligand pocket detection, BMC Bioinformatics 10(1) (2009) 168.
[29] M.S. Valdés-Tresanco, M.E. Valdés-Tresanco, P.A. Valiente, E. Moreno, AMDock: a versatile graphical tool for assisting molecular docking with Autodock Vina and Autodock4, Biology Direct 15(1) (2020) 12.
[30] S. Kim, J. Chen, T. Cheng, A. Gindulyte, J. He, S. He, Q. Li, B.A. Shoemaker, P.A. Thiessen, B. Yu, L. Zaslavsky, J. Zhang, E.E. Bolton, PubChem 2023 update, Nucleic Acids Research 51(D1) (2022) D1373-D1380.
[31] S. Zheng, W. Wang, J. Aldahdooh, A. Malyutina, T. Shadbahr, Z. Tanoli, A. Pessia, J. Tang, SynergyFinder Plus: Toward Better Interpretation and Annotation of Drug Combination Screening Datasets, Genomics Proteomics Bioinformatics 20(3) (2022) 587-596.
[32] G. Wu, Y. Zheng, H. Zhou, X. Hu, J. Liu, Y. Zhai, M. Zhu, L. Wu, J. Shentu, Safety and pharmacokinetics of dicloxacillin in healthy Chinese volunteers following single and multiple oral doses, Drug design, development and therapy 9 (2015) 5687-95.
[33] N. Li, S. Liu, H. Luo, A NEW METHOD FOR THE DETERMINATION OF THE FIRST AND SECOND CMC IN CTAB SOLUTION BY RESONANCE RAYLEIGH SCATTERING TECHNOLOGY, Analytical Letters 35(7) (2002) 1229-1238.
[34] S. Preus, DecayFit—Fluorescence Decay Analysis Software 1.3, FluorTools, http://www.fluortools.com (2014).
[35] A. Micsonai, É. Moussong, F. Wien, E. Boros, H. Vadászi, N. Murvai, Y.-H. Lee, T. Molnár, M. Réfrégiers, Y. Goto, Á. Tantos, J. Kardos, BeStSel: webserver for secondary structure and fold prediction for protein CD spectroscopy, Nucleic Acids Research 50(W1) (2022) W90-W98.
[36] A. Tao, Y. Huang, Y. Shinohara, M.L. Caylor, S. Pashikanti, D. Xu, ezCADD: A rapid 2D/3D visualization-enabled web modeling environment for democratizing computer-aided drug design, Journal of chemical information and modeling 59(1) (2018) 18-24.
[37] P. Buchwald, A Receptor Model With Binding Affinity, Activation Efficacy, and Signal Amplification Parameters for Complex Fractional Response Versus Occupancy Data, Frontiers in pharmacology 10 (2019) 605.
[38] C.G. Specht, Fractional occupancy of synaptic binding sites and the molecular plasticity of inhibitory synapses, Neuropharmacology 169 (2020) 107493.
[39] J. Corzo, Time, the forgotten dimension of ligand binding teaching, Biochemistry and molecular biology education : a bimonthly publication of the International Union of Biochemistry and Molecular Biology 34(6) (2006) 413-6.
[40] S. Kundu, ReDirection: an R-package to compute the probable dissociation constant for every reaction of a user-defined biochemical network, Frontiers in Molecular Biosciences 10 (2023).
[41] S.I. Berger, R. Iyengar, Network analyses in systems pharmacology, Bioinformatics 25(19) (2009) 2466-2472.
[42] M.R. Karim, M. Cochez, J.B. Jares, M. Uddin, O. Beyan, S. Decker, Drug-Drug Interaction Prediction Based on Knowledge Graph Embeddings and Convolutional-LSTM Network, Proceedings of the 10th ACM International Conference on Bioinformatics, Computational Biology and Health Informatics, Association for Computing Machinery, Niagara Falls, NY, USA, 2019, pp. 113–123.
[43] K. Han, P. Cao, Y. Wang, F. Xie, J. Ma, M. Yu, J. Wang, Y. Xu, Y. Zhang, J. Wan, A Review of Approaches for Predicting Drug–Drug Interactions Based on Machine Learning, Frontiers in pharmacology 12 (2022).
[44] F. Azuaje, Drug interaction networks: an introduction to translational and clinical applications, Cardiovascular Research 97(4) (2012) 631-641.
[45] A. Mahata, D. Sarkar, D. Bose, D. Ghosh, P. Das, N. Chattopadhyay, Photophysics and rotational relaxation dynamics of a β-carboline based fluorophore in cationic alkyltrimethylammonium bromide micelles, Journal of Colloid and Interface Science 335(2) (2009) 234-241.
[46] S. Matzinger, D.M. Hussey, M.D. Fayer, Fluorescent Probe Solubilization in the Headgroup and Core Regions of Micelles: Fluorescence Lifetime and Orientational Relaxation Measurements, The Journal of Physical Chemistry B 102(37) (1998) 7216-7224.
[47] S.R. Rai, A. Sarkar, A. Pandey, S. Dasgupta, I. Majumder, D. Das, D. Bose, M. Mukhopadhyay, Photometric Study of the Interaction of Zinc (II) Complexes of Schiff Bases with Cetyltrimethyl Ammonium Bromide, Macromolecular Symposia 388(1) (2019) 1900030.
[48] S. Berr, R.R.M. Jones, J.S. Johnson, Jr., Effect of counterion on the size and charge of alkyltrimethylammonium halide micelles as a function of chain length and concentration as determined by small-angle neutron scattering, The Journal of Physical Chemistry 96(13) (1992) 5611-5614.
[49] A.M. Tedeschi, L. Franco, M. Ruzzi, L. Paduano, C. Corvaja, G. D'Errico, Micellar aggregation of alkyltrimethylammonium bromide surfactants studied by electron paramagnetic resonance of an anionic nitroxide, Physical Chemistry Chemical Physics, 2003, pp. 4204-4209.
[50] J. Ognjenović, M. Stojadinović, M. Milčić, D. Apostolović, J. Vesić, I. Stambolić, M. Atanasković-Marković, M. Simonović, T.C. Velickovic, Interactions of epigallo-catechin 3-gallate and ovalbumin, the major allergen of egg white, Food Chemistry 164 (2014) 36-43.

[51] E. Gudgin, R. Lopez-Delgado, W.R.J.T.J.o.P.C. Ware, Photophysics of tryptophan in water, deuterium oxide and in nonaqueous solvents, The Journal of Physical Chemistry 87(9) (1983) 1559-1565.
[52] J.-M.G. Rodriguez, N.P. Hux, S.J. Philips, M.H. Towns, Michaelis–Menten Graphs, Lineweaver–Burk Plots, and Reaction Schemes: Investigating Introductory Biochemistry Students' Conceptions of Representations in Enzyme Kinetics, Journal of Chemical Education 96(9) (2019) 1833-1845.
[53] J.R. Lakowicz, Principles of fluorescence spectroscopy, Springer2006.
[54] M.D.d.A. Dantas, H.d.A. Tenório, T.I.B. Lopes, H.J.V. Pereira, A.J. Marsaioli, I.M. Figueiredo, J.C.C. Santos, Interactions of tetracyclines with ovalbumin, the main allergen protein from egg white: Spectroscopic and electrophoretic studies, International Journal of Biological Macromolecules 102 (2017) 505-514.
[55] Y. Liu, Y. Cai, D. Ying, Y. Fu, Y. Xiong, X. Le, Ovalbumin as a carrier to significantly enhance the aqueous solubility and photostability of curcumin: Interaction and binding mechanism study, International Journal of Biological Macromolecules 116 (2018) 893-900.